

EVALUATION OF THE EFFECT OF TURBID WATER IN CANALS ON UNDERWATER ULTRASONIC ROUGHNESS MEASUREMENTS

*Nozomu Urahata¹, Kenji Okajima¹

¹Graduate School of Bioresources, Mie University, Japan

*Corresponding Author, Received: 15 June 2023, Revised: 22 March 2024, Accepted: 25 March 2024

ABSTRACT: Abrasion occurs on the concrete surfaces of irrigation canals because of the flow of water and sand. Abrasion increases the roughness of the concrete surface. Increased roughness reduces water flow function. Underwater ultrasonic roughness measurements estimate roughness from the peak-to-peak strength of reflected underwater ultrasonic waves. However, the effect of turbid water flowing in a canal on peak-to-peak strength has been unclear. The objective of this study was to evaluate the effect of turbid water on underwater ultrasonic roughness measurements. The characteristics of the attenuation of the peak-to-peak strength of underwater ultrasonic waves were investigated as a function of the particle size and concentration of suspended solids. The suspended solids used in the experiments were kaolin with a particle size of 0.5 μm and alumina with particle sizes of 2, 4, and 8 μm . Peak-to-peak strength was measured as a function of the concentration of each particle size. The experimental results indicated that peak-to-peak strength was attenuated only with increasing concentrations of suspended solids and was not affected by particle size. A proposed correction equation for peak-to-peak strength took into consideration the concentration of suspended solids in turbid water. The coefficient of determination R^2 between this equation and measured data was as high as 0.98. Using this correction equation, peak-to-peak strength without turbidity could be calculated from peak-to-peak strength measured in turbid water. It is thus possible to make effective use of underwater ultrasonic roughness measurements in turbid water.

Keywords: Underwater ultrasonic waves, Peak-to-peak strength, Turbid water, Attenuation characteristics, Suspended solids

1. INTRODUCTION

Agricultural irrigation facilities such as dams, headworks, and irrigation canals in Japan are currently facing the problem of aging. Many of the facilities were constructed before the 1970s and are deteriorating. The total length of irrigation canals in Japan is approximately 400,000 km, including the terminus [1]. One of the deteriorations caused by the aging of irrigation canals is abrasion. Abrasion occurs on the concrete surfaces of canals because of the movement of water and sand, and reduces the water flow function in the canal by increasing the roughness of the concrete surface. The reduction in the water flow function decreases the speed of water flowing through the canal and raises the water level. Repairing the canal is necessary to prevent the progression of abrasion. In recent years, the tight financial condition has promoted stock management efforts to economically extend the service life of irrigation facilities by making appropriate repairs at the appropriate time. Quantitative roughness measurements are necessary to determine the appropriate time for canal repair, on the other hand, most methods of measuring the roughness of concrete surfaces in canals rely on visual evaluation, which is not a quantitative measurement method [2]. It has therefore been difficult to make repairs at appropriate times.

In general, the arithmetic mean roughness R_a is

used as an index for evaluating the roughness of concrete surfaces. Several methods have been proposed for measuring the roughness of water canals. A measurement method using a moulage gauge involves pressing a series of needles against the surface to read the roughness and convert it to a roughness value. This method obtains the roughness as a line at the measured place and is inexpensive and easy to measure. However, it requires labor for analysis [3]. A measurement method using a laser rangefinder reads unevenness and converts it to roughness by measuring the distance between the laser head and the measurement surface in 0.1 mm increments. This method obtains the roughness as a line at the measured place and is very accurate. However, measuring many concrete canals is time-consuming [4]. A measurement method using an aerial ultrasonic involves irradiation of a measurement surface with ultrasonic waves and estimates roughness from the peak-to-peak strength of the reflected waves. This method differs from a moulage gauge and a laser rangefinder in that it can obtain the roughness as a whole area of 200 mm in diameter at the measured place. Roughness measurement devices based on aerial ultrasonic technology are currently being developed [5, 6].

These measurement methods assume that there is no water in the canal during the non-irrigated period. It is therefore difficult to measure roughness in canals where water flows year-round, such as greenhouse

cultivation areas. In addition, it is not easy to stop the flow of water in a canal. A roughness measurement method using underwater ultrasonic waves has therefore been proposed. This method is based on estimating the arithmetic mean roughness R_a of a concrete surface from the peak-to-peak strength of reflected underwater ultrasonic waves [7]. It is possible to obtain roughness as a whole area in the same method as with the aerial ultrasonic method.

Previous studies of underwater ultrasonic roughness measurements [7] have examined only non-turbid water. The water that flows in irrigation canals is assumed to be turbid. In fact, the particle size of suspended solids in agricultural drainage canals has been reported to be about 7–8 μm , and in some cases, tens of μm [8, 9]. In addition, the concentration of suspended solids is reported to be several tens of mg/L to 100 mg/L, except during the period of ploughing and irrigating the fields, etc. [8], [10]. It has also been reported that the larger the particle size and concentration of suspended solids in water, the greater the attenuation of underwater ultrasonic waves [11]. However, the effect of turbidity on roughness measurements made by underwater ultrasonic methods has not been investigated. The objective of this study was therefore to evaluate the effect of turbidity on roughness measurements by underwater ultrasonic methods. This study investigated the characteristics of the attenuation of the peak-to-peak strength of underwater ultrasonic waves as a function of particle size and concentration of suspended solids. We also investigated use of an equation to correct underwater ultrasonic roughness measurements in turbid water.

2. RESEARCH SIGNIFICANCE

Previous studies that have proposed the use of underwater ultrasonic methods to measure the roughness of concrete surfaces [7] have not taken the turbidity of the water into consideration. The water flowing in irrigation canals is assumed to be turbid, and the effect of that turbidity on roughness measurements is a concern. Measurement of the roughness in actual irrigation canals will require investigation of the effect of the turbidity of the water flowing through the canals on underwater ultrasonic waves. The goal of this study was therefore to evaluate the effect of turbid water on underwater ultrasonic roughness measurements.

3. PRINCIPLE OF UNDERWATER ULTRASONIC ROUGHNESS MEASUREMENT

Roughness measurements using underwater ultrasonic methods are based on the phenomenon that the rougher the concrete surface, the more scattered waves are generated. The effectiveness of the method

has been confirmed in non-turbid water [7]. Underwater ultrasonic waves are first irradiated onto a concrete surface from an underwater ultrasonic sensor. The irradiated waves are then reflected from the concrete surface and received by the same sensor as reflected waves. The received reflected wave is converted to an electrical signal to obtain the peak-to-peak strength. Figure 1 shows the reflected wave of underwater ultrasonic waves and peak-to-peak strength. The peak-to-peak strength is the difference between the maximum and minimum voltages, and, as Figure 1 shows, the rougher the concrete surface, the smaller the peak-to-peak strength. The peak-to-peak strength is used to estimate the roughness of the concrete surface. However, in turbid water, the peak-to-peak strength has the possibility to be decreased because of suspended solids in the water. Therefore, this study investigates the effect of suspended solids on roughness measurement by underwater ultrasonic methods.

4. MATERIALS AND METHODS

4.1 Suspended Solids

We used kaolin (HYASHI PURE CHEMICAL IND., LTD.) with a particle size of 0.5 μm and alumina (The Association of Power Process Industry and Engineering, JAPAN) with particle sizes of 2, 4, 8, and 30 μm as the suspended solids. However,

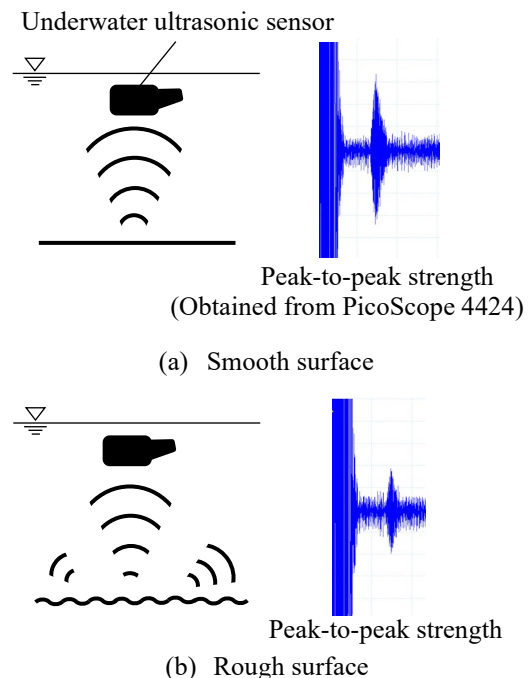


Fig. 1 The reflected wave of underwater ultrasonic waves and peak-to-peak strength.



Fig. 2 The underwater ultrasonic sensor used in the study

particle sizes of 30 μm were not suitable for the experiment because of severe sedimentation, even with sufficient stirring. Therefore, it was excluded from this study.

4.2 Underwater Ultrasonic Sensor

We used an underwater ultrasonic sensor (Hook Reveal 5 83/200 HDI (manufactured by Lowrance). This sensor is sold as a fish finder and is readily available. We used a personal computer oscilloscope PicoScope 4424 (Pico Technologies Inc.) to obtain peak-to-peak strength measurements. To stabilize the voltage, we used a stabilizing power supply STP3010D (Shenzhen SKY TOP POWER Technology Co., Ltd.) to convert the input voltage of 100 alternating current volts to the output voltage of 12 direct current volts.

4.3 Concrete Panels (Measurement Surface)

The rougher the measurement surface, the larger the scattered waves are because of unevenness, and the weaker the reflected waves. However, the presence of suspended solids has the possibility of weakening the reflected waves. We therefore investigated whether the attenuation of the peak-to-peak strength of underwater ultrasonic waves due to the roughness of the measurement surface was affected by the presence of suspended solids.

We used three types of concrete panels with different degrees of roughness as the measurement surfaces (panels (1)–(3) in Figure 3). These concrete

panels were made by pouring fresh concrete into formwork. Panel (1) was a smooth surface, and Panels (2) and (3) were rough surfaces. We simulated roughness in the case of panels (2) and (3) by applying a concrete retarder to the surface of the concrete after it had been poured into the formwork and then flushing the surface with water after a few hours to expose the aggregate. The panels were 300 mm long, 300 mm wide, and 28 mm thick. We measured the roughness index (R_a) with a moulage gauge. The roughness indices for panel (1), panel (2), and panel (3) were 0.05, 0.37, and 0.51 mm, respectively.

4.4 Experimental Methods

A schematic of the experiment is shown in Figure 4. The tank was filled with 164 L of tap water, and a concrete panel was placed on the bottom of the tank. Previous studies [7] have reported that when the distance between the underwater ultrasonic sensor and the concrete panel is 500 mm, the arithmetic mean roughness can be obtained with good accuracy, and the loss of the propagation of the underwater ultrasonic waves increases as the measurement distance increases. We placed the underwater ultrasonic sensor 400 mm directly above the concrete panel in this study. We prepared 18 solutions with different concentrations of suspended solids to investigate the effect of turbidity (Table 1). The concentrations ranged from 0 to 213 mg/L. For each concentration of suspended solids, peak-to-peak strength was first measured at 0 mg/L. Subsequently, suspended solids were added as indicated in Table 1, and a total of 18 peak-to-peak strength measurements were obtained. Each peak-to-peak strength was the average of 63 measurements. Peak-to-peak strength was measured immediately after the suspended solids had been added and after sufficient stirring.

4.5 Relationship Between Peak-to-peak Strength and Arithmetic Mean Roughness of Concrete Panels

The relationship between peak-to-peak strength and the R_a of the concrete panels measured in this study is shown in Figure 5. The peak-to-peak strength



Panel (1) $R_a = 0.05\text{mm}$



Panel (2) $R_a = 0.37\text{mm}$



Panel (3) $R_a = 0.51\text{mm}$

Fig. 3 Concrete panels

Table 1 Concentrations and total inputs of suspended solids

Total input (mg)	0	500	1000	1500	2000	3000
Concentration (mg/L)	0	3	6	9	12	18
Total input (mg)	4000	5000	6000	7000	8000	9000
Concentration (mg/L)	24	30	37	43	49	55
Total input (mg)	10000	15000	20000	25000	30000	35000
Concentration (mg/L)	61	91	122	152	183	213

values for each surface are those measured in non-turbid water, that is, at 0 mg/L. Because the experiment was conducted with different suspended solids per surface, four peak-to-peak strengths were measured at 0 mg/L, and the average of these peak-to-peak strengths was plotted. The coefficient of determination R^2 (0.91) between arithmetic mean roughness and peak-to-peak strength was high.

5. METHODS FOR EVALUATING THE EFFECT OF SUSPENDED SOLIDS ON UNDERWATER ULTRASONIC WAVES

5.1 Measured Attenuation Ratio (A_m)

We assessed the effect of suspended solids on underwater ultrasonic waves by examining the attenuation of peak-to-peak strength. The peak-to-peak strengths varied as a function of the roughness of the panel. We therefore used the measured attenuation ratio based on peak-to-peak strength measured at 0 mg/L as the evaluation index. We expressed the measured attenuation ratio A_m with equation (1).

$$A_m = \frac{I}{I_0} \quad (1)$$

A_m : measured attenuation ratio, I_0 : peak-to-peak strength (V) at a suspended solids concentration of 0 mg/L, I : peak-to-peak strength (V) at each concentration of suspended solids. If the measured attenuation ratio was less than 1, the peak-to-peak strength had been attenuated.

5.2 Calculated Attenuation Ratio (A_c)

The attenuation ratio calculated in a previous study [11] was expressed by equation (2).

$$A_c = e^{-2\alpha r} \quad (2)$$

A_c : calculated attenuation ratio, r : round-trip measurement distance (mm), α : attenuation coefficient. Then, α was described as follows:

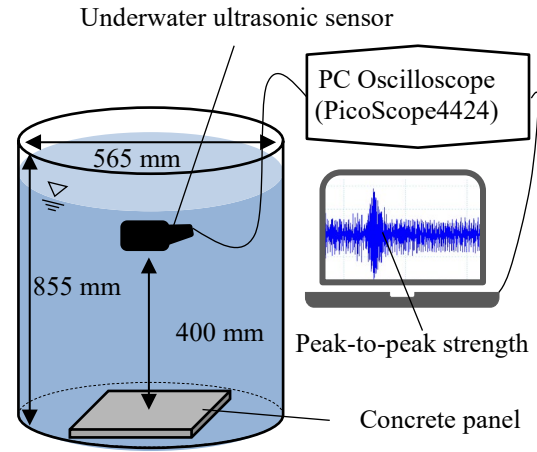


Fig. 4 Schematic of the experiment

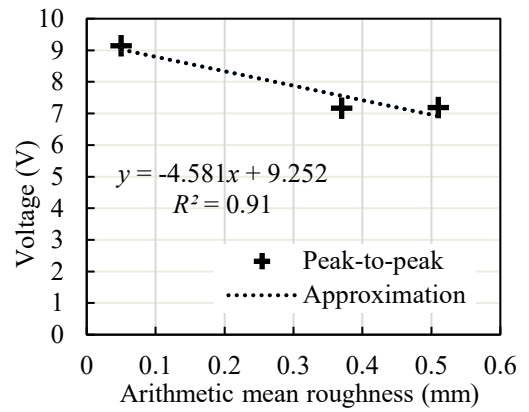


Fig. 5 Relationship between peak-to-peak strength and arithmetic mean roughness

$$\alpha = \alpha_w + \alpha_1 + \alpha_2 \quad (3)$$

α_w : absorption by seawater, α_1 : absorption by particle radius, α_2 : scattering by particle radius.

The absorption α_w by seawater was described as follows:

$$\alpha_w = \left[\frac{1.865 f_t f}{f_t^2 + f^2} + \frac{2.68 f}{f_t} \right] \quad (4)$$

$$f_t = 21.9 \times 10^6 \frac{1520}{273+T}$$

f : frequency of ultrasonic wave in water (kHz), f_t : relaxation frequency (kHz), T : water temperature ($^{\circ}\text{C}$), S : salinity.

The absorption α_1 due to particles was described as follows:

$$\alpha_1 = (10 \log e^2) \frac{Mk(\sigma-1)^2}{2\rho_s} \left[\frac{S}{S^2+(\sigma+\delta)^2} \right] \quad (5)$$

$$\sigma = \frac{\rho_s}{\rho_w}, \quad \delta = \frac{1}{2} \left[1 + \frac{9}{2\beta d} \right], \quad s = \frac{9}{4\beta d} \left[1 + \frac{1}{\beta d} \right],$$

$$\beta = \left[\frac{kc}{sv_w} \right]$$

M : concentration (mg/L), k : wavenumber (m^{-1}), ρ_s : particle density (g/cm^3), ρ_w : density of water (g/cm^3), d : particle radius (m), v_w : kinematic viscosity (m^2/s), c : propagation speed of ultrasonic wave in water (m/s).

The scattering α_2 by particles was described as follows:

$$\alpha_2 = (10 \log e^2) \frac{3MX^2}{4d\rho_s} \quad (6)$$

$$X = \frac{1.1(4/3)k_a x^4}{[1+1.3x^2+(4/3)k_a x^4]}, \quad x = kd, \quad k_a = 0.18$$

In this study, f was 83 kHz, f_t was 116 kHz, T was 20°C , S was 0, M and d was the particle radius used in that experiment. Other assigned values were $k = 347.67$, $\rho_w = 998.2 \text{ kg}/\text{cm}^3$, $v_w = 1.004 \times 10^{-6} \text{ m}^2/\text{s}$, and c for $\rho_s = 2600 \text{ kg}/\text{m}^3$ for kaolin and $4000 \text{ kg}/\text{m}^3$ for alumina.

6. RESULTS AND DISCUSSION

The results for a particle size of $0.5 \mu\text{m}$ are shown in Figure 6, for $2 \mu\text{m}$ in Figure 7, for $4 \mu\text{m}$ in Figure 8, and for $8 \mu\text{m}$ in Figure 9.

The results for particle sizes of 0.5 , 2 , and $8 \mu\text{m}$ showed a similar trend, with attenuation of approximately 10% . At a particle size of $4 \mu\text{m}$, the trend was different.

6.1 Difference in Roughness of Measurement Surface

Figures 6, 7, and 9 show that the attenuation at particle sizes of 0.5 , 2 , and $8 \mu\text{m}$ followed a similar trend, regardless of the roughness of the panel. Figure 8 shows that the trend differed for the particle size of $4 \mu\text{m}$, and the attenuation ratio increased in the order panel (3), panel (1), and panel (2).

The rougher the surface, the weaker the reflected wave. If the weaker reflected wave was more affected by suspended solids, the attenuation ratio should have increased from panel (3), to panel (2), to panel (1), in that order. However, no such trend was observed. It was therefore clear that the difference in roughness

did not affect the attenuation of the peak-to-peak strength of underwater ultrasonic sound due to suspended solids.

6.2 A_m Results at $4 \mu\text{m}$ Particle Size

Figure 8 shows that the A_m results at a particle size of $4 \mu\text{m}$ varied. The vertical axis of the graph in Figure 8 is enlarged and shown in Figure 10. Figure 10 shows that the A_m in panel (2) increased sharply at a suspended solids concentration of $3 \text{ mg}/\text{L}$, while it decreased sharply in panel (3). Equation (1) indicates that if the measured value of I_0 is smaller than it should be, A_m becomes larger. Conversely, A_m becomes smaller when I_0 is larger. If the values above a suspended solids concentration of $3 \text{ mg}/\text{L}$ are considered as a standard, panel (2) shows an attenuation of about 9% , and panel (3) shows an attenuation of about 14% . These percentages are similar to the other measurements at particle sizes of 0.5 , 2 , and $8 \mu\text{m}$. It is therefore possible that the results for the particle size of $4 \mu\text{m}$ was due to mismeasurement of I_0 in equation (1), and that the trend of attenuation was the same for all measurement panels.

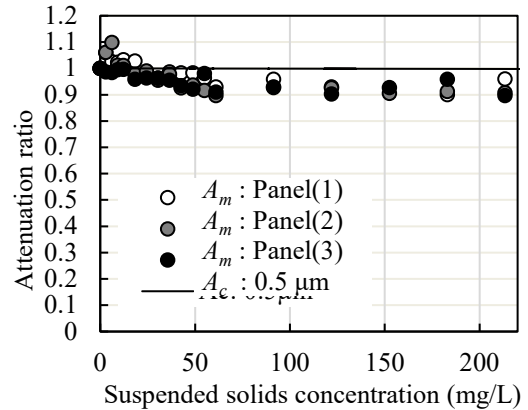


Fig. 6 Attenuation ratio of particle size $0.5 \mu\text{m}$

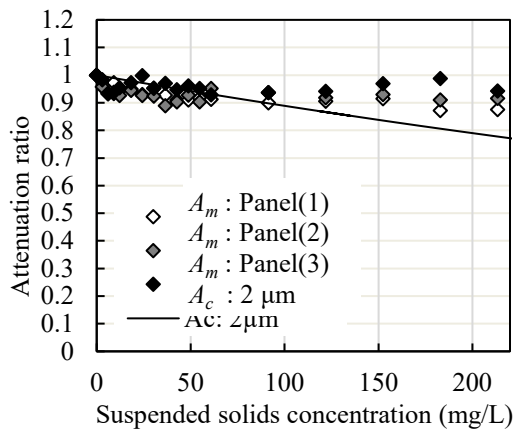


Fig. 7 Attenuation ratio of particle size $2 \mu\text{m}$

6.3 Difference between A_m and A_c

The measured attenuation ratio A_m and the calculated attenuation ratio A_c gave different results. For A_c , the larger the particle size, the larger the attenuation; however, no such trend was observed in the case of A_m . A possible reason for this difference in results is differences in the characteristics of the devices used in a previous study [11] and in this study. In the future, it will be necessary to investigate the causes of these differences. In the previous study, an Acoustic Doppler Current Profiler (ADCP) was used; in this study, we used a fish finder. Both devices have in common the use of underwater ultrasonic technology. The ADCP is used mainly to observe the flow of water, which requires the capture of small reflections from water particles and suspended solids in the water.

6.4 Statistical Analysis of Measured Attenuation Ratios

The results of our experiments showed that the measured attenuation ratios A_m were similar, regardless of the particle size of the suspended solids. We therefore hypothesized that the attenuation of underwater ultrasonic waves was independent of particle size. To test this hypothesis, we performed a statistical analysis using the non-parametric Kruskal–Wallis (KW) test. This test was chosen because the results for the 4 μm particle size showed more variability than the results for the other particle sizes, possibly indicating that dispersion was not uniform among the particle sizes. If this hypothesis is correct, there should be no significant difference in the attenuation between particle sizes. The significance level was set at 5%, and data from the four groups classified by particle size were compared at one concentration. For example, the 0.5 μm particle size group included the three A_m shown in panels (1), (2), and (3). The KW test results in a test statistic, H . This H approximately follows a χ^2 distribution with $k - 1$ degrees of freedom. Because there were four particle sizes of suspended solids and the statistical analysis was based on four groups, the degrees of freedom were 3. From the χ^2 distribution with 3 degrees of freedom, there is a significant difference when $H > 7.815$ and no significant difference when $H \leq 7.815$ at the 5% level of significance. Table 2 shows the results of the statistical analysis.

Table 2 shows that there was no significant difference in attenuation ratio between particle size at any of the concentrations. We therefore assumed that there was no difference in the attenuation of underwater ultrasonic waves between particle sizes and that the attenuation was related only to the concentration. All 12 A_m values obtained for each concentration were therefore averaged to represent the average measured attenuation ratio.

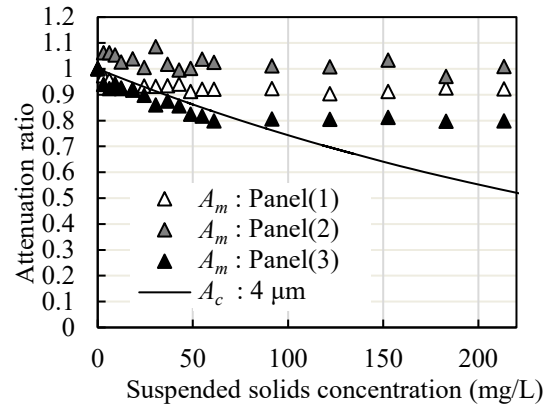


Fig. 8 Attenuation ratio of particle size 4 μm

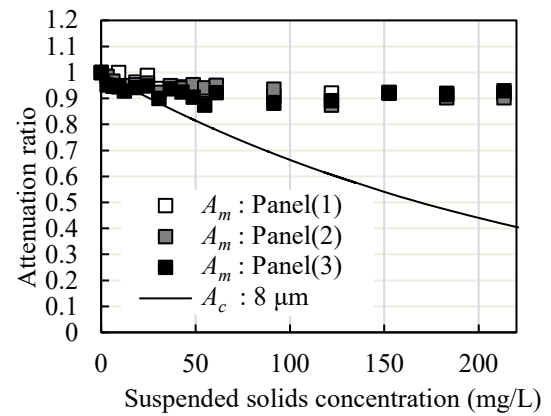


Fig. 9 Attenuation ratio of particle size 8 μm

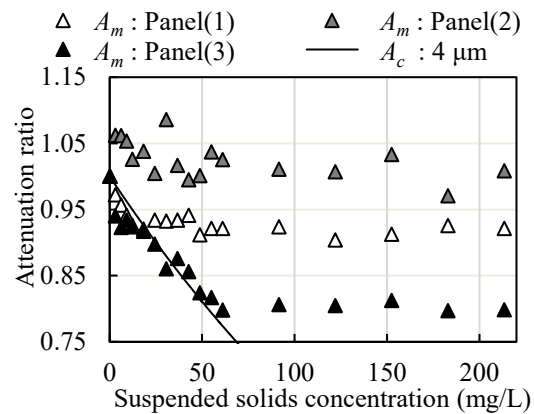


Fig. 10 Results at 4 μm with enlarged vertical axis

6.5 Correction Equation of Peak-to-peak Strength

We developed an equation to correct the peak-to-peak attenuation of underwater ultrasonic waves for the concentration of particles. First, we developed an approximation for the average of the 12 A_m values. For the approximation, we used the equation of the Verhulst model. Figure 11 shows the average of the 12 A_m values and the approximation we developed.

Table 2 The results of the statistical analysis

Concentration (mg/L)	0	3	6	9	12	18
Test statistics H	0.000	3.923	5.769	4.231	4.641	2.590
Concentration (mg/L)	24	30	37	43	49	55
Test statistics H	1.256	4.744	3.308	0.744	0.487	1.103
Concentration (mg/L)	61	91	122	152	183	213
Test statistics H	2.077	1.513	1.974	1.212	0.077	0.128

The Verhulst model equation, which was the basis of the approximation, has the characteristic of converging to a constant value after first showing an exponential increase or decrease [12]. The average of 12 A_m values plotted in Figure 11 decreased exponentially up to a concentration of 50 mg/L and then converged to ~ 0.92 . We therefore choose the Verhulst equation as an approximation. Equation (7) shows the Verhulst model equation with variables modified for this study and fitted to the average of the 12 A_m .

$$N = \frac{0.916}{1 - 0.084e^{-0.031t}} \quad (7)$$

N : attenuation ratio, t : concentration of suspended solids.

The coefficient of determination between Equation (7) and the average of the 12 A_m was high, 0.98. As Figure 11 shows, the characteristics of the average of 12 A_m values were captured well. Equation (7) was therefore appropriate for estimating attenuation ratios from suspended solids concentrations. This equation expressed the attenuation ratio N as a function of the concentration t of suspended solids. Assuming that the peak-to-peak strength measured at a certain concentration t is I_t , equations (1) and (7) could therefore be summarized in equation (8) below.

$$\frac{I_t}{I_0} = N \quad (8)$$

By transforming equation (8), I_0 can be expressed as a function of I_t measured in turbid water and the concentration t of the turbid water. Equation (9), the correction equation from the measured peak-to-peak strength I_t to I_0 , is thus obtained.

$$I_0 = \frac{I_t}{N} = \frac{1 - 0.084e^{-0.031t}}{0.916} \times I_t \quad (9)$$

Using this correction equation, the peak-to-peak strength I_t measured in turbid water can be converted to I_0 measured at a concentration of 0 mg/L. Previous studies have shown that arithmetic mean roughness can be obtained from peak-to-peak strength, as measured in non-turbid water, i.e., I_0 . It is therefore

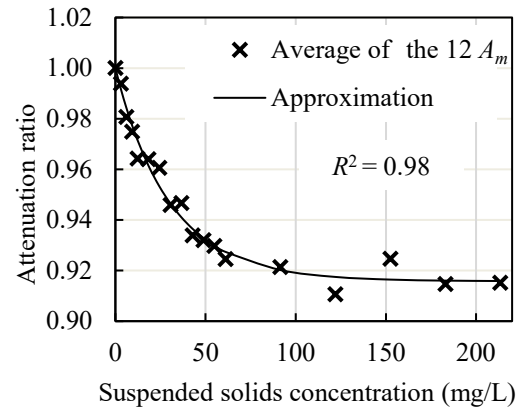


Fig. 11 Actual values and the approximation for the average measured attenuation ratio

possible that roughness can be measured in turbid water using this equation.

7. CONCLUSIONS

The objective of this study was to evaluate the effect of turbid water on underwater ultrasonic roughness measurements. In the experiment, the peak-to-peak strength attenuation of underwater ultrasonic waves due to the particle size and concentration of suspended solids was investigated. We found that differences in roughness were not related to the attenuation of the peak-to-peak strength of underwater ultrasonic waves due to suspended solids. For suspended solids with particle sizes of 0.5, 2, 4, and 8 μm , peak-to-peak strength attenuation was similar, regardless of particle size. Statistical analysis showed no significant differences in measured attenuation ratios between particle sizes. For particle sizes from 0.5 to 8 μm , the attenuation of peak-to-peak strength was found to be independent of the particle size of the suspended solids. Only the concentration was found to be relevant for the attenuation. The approximation for the average measured attenuation ratio was found to have a high coefficient of determination and high agreement. Using the correction equation, peak-to-peak strength affected by suspended solids could be corrected and

converted to peak-to-peak strength in non-turbid water. It is therefore possible that an underwater ultrasonic roughness measurement obtained in turbid water is effective for particle sizes range 0.5–8 μm and concentrations of 0–213 mg/l. Future work will be needed to verify the effect of suspended solids in canals at certain times of the year when large particle sizes occur, which could not be considered in this study.

8. REFERENCES

- [1] Ministry of Agriculture, Forestry and Fisheries, in Japan, Guidance for Functional Diagnosis of Agricultural Water Utilization Facilities, 2023, pp. 2,5. [online] <https://www.maff.go.jp/j/nousin/mizu/sutomane/attach/pdf/kinouhozen-201.pdf> [Accessed 9 June 2023]
- [2] Ministry of Agriculture, Forestry and Fisheries, in Japan, Guidance for Functional Diagnosis of Agricultural Water Utilization Facilities (open channel), 2016, pp. 13, 49-51. [online] <https://www.maff.go.jp/j/nousin/mizu/sutomane/attach/pdf/kinouhozen-20.pdf> [Accessed 9 June 2023]
- [3] Kawakami A., Asano I., Mori M., Kawabe S. and Tokashiki M., Abrasion Measurement Method Using a Profile Gauge, The Japanese Society of Irrigation, Drainage and Rural Engineering, vol. 85, No. 1, 2017, pp. 77-84.
- [4] Asano I., Tokashiki M., Mori M. and Nishihara M., Development of Erosion Monitoring System on Laser Displacement Meter for Cementitious Surface Coating Method, The Japanese Society of Irrigation, Drainage and Rural Engineering, Vol. 82, No. 5, 2014, pp. 285-296.
- [5] Okajima K., Nagaoka S., Ishiguro S., Ito R., Watanabe K. and Ito T., Measurement of the Roughness of the Concrete Surface by the Peak to Peak Value of the Aerial Ultrasonic Wave, The Japanese Society of Irrigation, Drainage and Rural Engineering, Vol. 84, No. 3, 2016, pp. 233-240.
- [6] Nagaoka S., Islam M.R., Okajima K., Ito R., Watanabe K. and Ito T., Evaluated of Attenuation of Ultrasonic Wave in Air to Measure Concrete Roughness Using Aerial Ultrasonic Sensor, International Journal of GEOMATE, Vol. 14, Issue 42, 2018, pp. 158-163.
- [7] Nagaoka S., Okajima K., Ito R., Islam M.R. and Watanabe K., Development of Underwater Ultrasonic Wave Sensor for Measuring Concrete Surface Roughness, The Japanese Society of Irrigation, Drainage and Rural Engineering, Vol. 87, No. 1, 2019, pp. 91-97.
- [8] Sato N., Hosihino K., Osawa K. and Hirai H., Physico-chemical properties of paddy soils suspended in agricultural drainage water flowing into Lake Inawashiro during the period between puddling and transplanting, Journal of the science of soil and manure, Japan Vol. 84, No. 6, 2013, pp. 473-477.
- [9] Matsui H. and Sunaga Y., Observation and Application of L-Q Equation for Suspended Sediment Runoff from Paddy Fields, Ishigaki Island, Okinawa, Journal of Japan Society of Civil Engineers, ser. B1 Hydraulic Engineering, Vol. 69, No. 4, 2013, pp. 955-960.
- [10] Sunaga Y., Matsui H. and Osawa K., Temporal Change in Particle Size Distributions of Suspended Solids Discharged from Paddy Fields, The Japanese Society of Irrigation, Drainage and Rural Engineering, Vol. 85, No. 2, 2017, pp. 113-119.
- [11] Arai R., Nakatani N. and Okuno T., Measurement Method of Turbidity Depth Profile using ADCP for Monitoring of Coastal Sea Area, Journal of the Japan Society of Naval Architects and Ocean Engineers, Vol. 7, 2008, pp.23-30.
- [12] Burghes D. and Borrie M., Modelling with Differential Equations, Ellis Horwood Ltd, Publisher, 1981, pp. 1-172.

Copyright © Int. J. of GEOMATE All rights reserved, including making copies, unless permission is obtained from the copyright proprietors.
